# 7.6 PERFORMANCE OF THE NEW FOUR-DIMENSIONAL LIGHTNING SURVEILLANCE SYSTEM (4DLSS) AT THE KENNEDY SPACE CENTER/CAPE CANAVERAL AIR FORCE STATION COMPLEX

Martin J. Murphy*, Kenneth L. Cummins, Nicholas W.S. Demetriades
Vaisala Inc.
Tucson, AZ

William P. Roeder
45th Weather Squadron
Patrick AFB, FL

## 1. Introduction

The Cape Canaveral Air Force Station and NASA Kennedy Space Center (CCAFS/KSC) complex is the busiest space launch center in the U.S. It also is near the area with the highest lightning frequency in the U.S., with a cloud-to-ground (CG) lightning flash density exceeding 9 flashes/km$^2$/year (Orville and Huffines, 2001), with local measurements of 14 flashes/km$^2$/year. The combination of the unique operational requirements, large number of personnel working outdoors, expensive equipment protection requirements, and high lightning frequency make lightning one of the most critical weather phenomena at CCAFS/KSC.

A review of CCAFS/KSC operations is given in Bellue et al. (2006) and Harms et al. (2003). These include pre-launch and launch operations weather support, which is the responsibility of the Air Force's 45th Weather Squadron (45WS). In-flight and landing weather to the Space Shuttle is provided by the NWS Spaceflight Meteorology Group (Brody et al., 1997). Day-to-day operations and pre-launch work involves a lot of outdoor activity, sensitive equipment, and hazardous materials. To protect personnel and equipment, the 45WS is responsible for issuing lightning watches and warnings for 14 sites in and around the CCAFS/KSC complex, at Patrick AFB, and at Melbourne airport. In addition, prior to and during any launch or landing, special precautions are taken to avoid the threat posed by both natural and rocket-triggered lightning. These precautions are spelled out in the lightning Launch Commit Criteria (LCC), as discussed in more detail by Roeder and McNamara (2006).Two of the main lightning sensing systems used by the 45WS in both day-to-day and launch/landing operations are the Lightning Detection and Ranging (LDAR; Lennon and Maier, 1991) system and the Cloud-to-Ground Lightning Surveillance System (CGLSS; Boyd et al., 2005). LDAR is an array of 7 VHF antennas that sense impulsive emissions from lightning in the frequency range of approximately 60-66 MHz. Such emissions are produced in abundance by the processes of breakdown and channel formation in both cloud lightning and CG flashes. The abundance of these emissions, together with the free-space propagation of VHF signals, allows the system to produce full 3-D spatial mapping of lightning discharge activity. The CGLSS is a wide-band LF/VLF system consisting of the same IMPACT sensors used in the U.S. National Lightning Detection Network (NLDN; Biagi et al. 2007). The CGLSS is sensitive primarily to the return strokes in CG flashes, which are the sources of the strongest LF and VLF emissions in lightning discharges. Together these two

* *Corresponding author:* Martin J. Murphy, Vaisala Inc., 2705 E. Medina Rd., Tucson, AZ 85706.
martin.murphy@vaisala.com

systems provide a complete representation of the lightning activity at KSC/CCAFS.

The LDAR and CGLSS systems have limitations in terms of their supportability and maintainability. The LDAR system consists of a mix of legacy equipment from the original system and from a partial update of the hardware that processes the raw, analog sensor data. Data from the CGLSS sensors is processed on a legacy central processing system that can no longer be supported. In addition, due to the limited computational capability of the CGLSS central processor, the data stream from CGLSS has to be limited to just the first return stroke in each CG flash. This is a limitation, given that it is well known that many CG flashes contact ground in more than one location and that those locations can be separated by several km (Valine and Krider, 2002; Thottappillil et al. 1992).

In order to make both LDAR and CGLSS more supportable, CCAFS/KSC has recently upgraded both systems. The VHF system has been completely upgraded with new sensors and a central processor. The new VHF system is called the Four-Dimensional Lightning Surveillance System (4DLSS). The new 4DLSS central processor is also capable of processing the CGLSS sensor data at the same time, and moreover, it can produce the full CG stroke data, rather than just the first stroke, in real time. Thus, the combined, upgraded 4DLSS and CGLSS are better able to satisfy the critical requirements of the 45WS for space launch operations support. In this paper, we describe the 4DLSS system architecture, modeled performance, and performance validation. We also discuss the added benefit of having the full CG stroke data set available from the new central processor.

## 2. 4DLSS network architecture

The 4DLSS consists of nine sensors at the locations shown in Fig. 1. The seven sensor sites of the original LDAR network are also shown in Fig. 1 for reference. Note that the new sites create a baseline about 2.5 times wider than the original LDAR. This is known to reduce the radial location errors in a VHF time-of-arrival system proportional to the inverse square of the sensor baseline (Thomas et al. 2004). There are several reasons why the 4DLSS sensors can be separated by a larger distance than the original LDAR sensors. The first is that the sensors do not transmit analog signals back to a central station, as in the original LDAR system. Given that restriction, the original LDAR required that the remote sensors have line-of-sight communication to the central station. In addition, the 4DLSS location algorithm does not require that all sensors lie on the same plane, as did the original LDAR location algorithm. Figure 2 shows a model estimate of the horizontal (2-D) location accuracy of 4DLSS given an RMS timing error of 75 nsec. This expected random time error value is based on the sensors' individual timing precision of 50 ns and the accuracy of the GPS timing.

Figure 3 summarizes the model estimate in Fig. 2 in the form of a simple location accuracy versus distance plot from the center of the 4DLSS network. As one goes outside the perimeter of the network, the largest component of the location error lies in the radial (distance) direction. Our location accuracy values for 4DLSS always measure the largest component of the error, and therefore, the model estimate in Fig. 2 is inherently looking primarily at radial errors for locations outside the network. Thomas et al. (2004) predict that radial location errors are quadratic in distance from the center point between two sensors. Our projections are very consistent with a quadratic function of distance from the center of the network, which agrees with theory.

Figure 4 shows a model estimate of the geographical flash detection efficiency

(DE) of 4DLSS in the CCAFS/KSC area. Individual lightning flashes typically produce tens to hundreds of VHF emissions (hereafter, "VHF sources"). Given the abundance of sources per flash, it is reasonable to estimate the flash detection efficiency of the system by first making an estimate of the source detection efficiency (albeit with attendant uncertainties) and then using that together with a conservative value for the number of sources per flash (e.g., 20 or 50). This is how the model estimate in Figure 4 was made. In the interior of the 4DLSS network, the DE for individual VHF sources is estimated to be about 40-50%, which gives a flash DE of essentially 100%. This matches the legacy LDAR performance, which was a requirement for 4DLSS.

Figure 5 summarizes Fig. 4 as a DE-vs-distance plot from the center of the 4DLSS network. The received power at each sensor from a VHF source of a particular power level decreases as the inverse square of distance, but because of the interacting effects of the natural distribution of source powers and the number of sources in a flash, there is no simple, theoretical framework against which to model the fall-off in flash DE as a function of distance. Nevertheless, outside of the region from 0-50 km where flash DE is approximately constant, an empirical fit to the DE fall-off vs distance is quadratic but dominated by the linear term.

## 3. 4DLSS Performance Analysis

### *3.1 Flash Detection Efficiency*

We conducted two types of analysis of the flash detection efficiency of the 4DLSS by comparison with original LDAR. The first method was a simple, manual flash count that was applied at times when storms were isolated and produced discrete flashes at a relatively low rate. For more complicated storm situations, we developed an automated DE analysis algorithm in which we broke the entire data sets (one for LDAR, one for 4DLSS) into 0.2-second intervals and counted the sources detected by each network in 10X10 km grid cells in each 0.2-second interval. This gave us a three-dimensional grid (10X10 km spatial grid and a large number of 0.2-sec time intervals) for each network. We first compared the source counts from each network in each 3D grid cell individually. To avoid isolated 1- and 2-source “events” (likely outliers), we only counted those 3D grid cells with more than 2 sources detected by either network. When we found a 3D grid cell that had more than 2 sources in one network’s data but 2 or fewer in the other network’s, we then looked at nearest-neighbor grid cells, +/- 1 cell in each of the two spatial dimensions as well as in the time dimension. The process is illustrated in Figure 6. If we found a neighboring 3D cell that had more than 2 sources in the second network’s grid, we considered that to be a “match” for the original 3D cell in the first network’s grid. If we found that we could not match a neighboring 3D cell in the second network to the original 3D cell in the first network, then the first network’s event was considered undetected by the second network. The automated algorithm was first tested side-by-side with the manual flash count method for one case, and then we applied the automated algorithm to additional, more complex storm situations.

The results of the DE analysis are summarized in Table 1 for storms that occurred on 6 May and 2 August 2007. Storms on 2 Aug. produced low flash rates, so only the manual flash count procedure was required to analyze DE. The much larger and more complicated storm situation on 6 May was broken down into smaller time intervals, some of which had low enough flash counts for a manual analysis and some of which did not. The "relative detection efficiency" given in Table 1 refers to the 4DLSS detection efficiency relative to original LDAR. These values range from 95% to 109%. The values greater than 100% correspond primarily to times when storms

were at greater distance from the network. This suggests that having two more sensors in 4DLSS, together with the wider sensor separation, provides for improved DE at longer distance from the network.

Personnel from 45 WS conducted extensive subjective comparisons between 4DLSS and LDAR during the summer 2007 lightning season. The 4DLSS had about 140% of the sources of LDAR overall. The lightning events depicted by 4DLSS and LDAR showed excellent spatio-temporal correlation. The reduced radial location errors of 4DLSS made the cellular structure of thunderstorms and branched structure of individual lightning flashes much more obvious. Finally, LDAR occasionally depicted aircraft flying through clouds. This was never depicted on 4DLSS despite over a dozen aircraft signatures on LDAR. This is attributed to the better noise reduction/quality control algorithm of 4DLSS which requires a source to be above a threshold at five or more of the nine 4DLSS sensors for a valid position to be computed. The emissions from electrostatic discharges of planes flying though clouds are apparently numerous but weak and fail to meet the signal strength threshold across five sensors--another indirect benefit of the wider baseline of 4DLSS. Figures 7a-7b shows an example of all of the aforementioned effects. These figures both cover the period from 20:55-21:00 Z on 21 September 2007, with Fig. 7a showing the original LDAR data and 7b showing 4DLSS. This time period includes aircraft emissions observed by LDAR but not 4DLSS and shows the improved location accuracy of 4DLSS. Note especially the more distant storm whose VHF sources are very spread out in the LDAR plot. The total number of sources in the 4DLSS plot is 22% higher than in LDAR (30228 vs. 24854).

Table 1. Summary of detection efficiency analysis. Method = "M" for manual flash count, "A" for automated algorithm. Relative DE refers to 4DLSS flash count relative to original LDAR flash count. All dates are 2007.

| Date | Time | Method | Rel. DE % |
|---|---|---|---|
| May 6 | 1800-1830 | M | 95.3 |
| May 6 | 1800-1830 | A | 96.4 |
| May 6 | 1830-1845 | A | 95.2 |
| May 6 | 1845-1900 | A | 96.0 |
| May 6 | 1900-1915 | A | 98.1 |
| May 6 | 2000-2015 | A | 99.6 |
| May 6 | 2015-2030 | A | 100 |
| May 6 | 2030-2045 | A | 104 |
| May 6 | 2045-2100 | A | 111 |
| May 6 | 2100-2115 | A | 102 |
| May 6 | 2115-2130 | A | 105 |
| Aug. 2 | 2 cells (35 min total) | M | 100 |

*3.2 Location Accuracy*

The location accuracy of 4DLSS was also verified using two different methods. The primary method was to compare the chi-square distribution for located sources to a theoretical chi-square distribution assuming the same random timing error as used in our model-based estimate of location accuracy. In addition to this, we also made a number of comparisons of

individual flashes located by 4DLSS and original LDAR in order to verify that the same essential flash structure was being shown by both systems.

Figure 8 shows the analysis of the chi-square distributions using data from a 30-minute period on 25 December 2006. This chi-square analysis was done for lightning events detected by all of the 8 sensors that were operational at that time. The observed chi-square distribution was computed using a 75-nsec RMS timing error We also show the theoretical distribution that best fits the data in Fig. 8. The theoretical distribution also has a random timing error of 75 nsec. This confirms that the modeled location accuracy of the network shown in Figure 2 is in fact consistent with the true performance of the network.

Figures 9-11 show several samples of flashes as depicted by 4DLSS and original LDAR. The blue plot symbols show original LDAR data, and the red symbols show 4DLSS. These examples, and many other similar flashes that we analyzed in the same way, show a great deal of consistency between the flash structures seen by both networks. This demonstrates that, even though each system individually may have a relatively low detection efficiency for VHF sources, they detect and locate sources that depict the same channel structure within the flash. The tendency for each system to be biased toward higher-amplitude VHF sources probably contributes to this consistency. The consistent depiction of flash structures satisfies a critical end-user requirement. Note that we typically find more scatter in the original LDAR data, especially at distances of 50-100 km from the CCAFS/KSC complex. This is a manifestation of the degraded location accuracy given by the shorter-baseline LDAR system relative to 4DLSS. The location acuracy within the 4DLSS network, which encompasses virtually all the operations supported by 45 WS, is about 100 m. This matches the performance of LDAR, which was a requirement of the 4DLSS system.

The location accuracy effects seen above in Figures 9-11 also manifest themselves in storm-level features. Figures 12a and 12b compare 4DLSS and original LDAR data for a 5-minute period on 21 September 2007. Note in Figure 12a that a couple of small-scale gaps in the flash activity are resolvable in the 4DLSS data at the southwest end of one of the cells (see arrow in Figs 12a-12b). This same feature is washed out in the original LDAR data due to the poorer location accuracy (Fig. 12b). In particular, a possible ‘lightning hole’ was noted in the 4DLSS, and that thunderstorm subsequently went on to generate tornadoes. Lightning holes are one lightning signature that recently has been suggested as a possible severe thunderstorm precursor (e.g. Lang et al. 2004).

## 4. CGLSS Stroke Data

As noted previously, CG flashes frequently contact ground in more than one location. This has important consequences for lightning safety applications, which are one of the critical concerns of the 45WS during everyday operations at KSC/CCAFS. In addition, one of the most important purposes of the legacy CGLSS was to help the engineers at KSC/CCAFS evaluate the likelihood of damage to satellite and launch vehicle electronics. While most of the launch pads have lightning protection systems to protect against direct lightning strikes, nearby CG lightning can still cause damage to delicate electronics via electromagnetic pulse and induced currents (Roeder et al., 2005). Different levels of tests of the electronics are done depending on how close a CG lightning stroke is to the launch pad and how strong it is. These tests cost funds and time to perform and can cause delays in the launch schedule. The legacy central processor for the CGLSS had the

capability of calculating positions for all strokes, but this capability could not be enabled in real time without slowing down the processing to an unacceptable level during high lightning-rate situations. This problem has been alleviated in the new central processor, and the CGLSS system is now producing real-time data on all detected CG strokes. The difference between receiving information on all strokes and receiving just first-stroke data is shown in Figure 13. This figure shows the VHF sources detected by 4DLSS in several discharges (small dots), including a long, horizontal flash, together with the CG return strokes (triangles). The order of the three strokes is shown in the figure (1,2,3). Stroke 3 is separated from the first two by 7.6 km and 7.3 km, respectively. This flash illustrates the importance of CG stroke information for the lightning warning and protection application.

The 4DLSS performance was also compared to the legacy CGLSS by 45 WS personnel during the summer of 2007. The 4DLSS had about 250% of the return strokes of the legacy CGLSS processor. This was roughly as expected given the difference between displaying all strokes versus just the first stroke in each flash.

## 5. Conclusions

We have summarized the upgraded 4DLSS VHF lightning detection network at the CCAFS/KSC and its performance characteristics relative to models and relative to the original LDAR system. We have shown that the 4DLSS has improved location accuracy at moderate distance from CCAFS/KSC over the original LDAR system. We have also shown what is inferred to be improved flash detection efficiency at longer distances. In addition, the integration of the CGLSS sensors into a new central processor has allowed 45WS to have access to real-time data on all detected CG strokes. This is an important contribution to the lightning safety and protection responsibilities that the 45WS has on a daily basis. Together, the 4DLSS and CGLSS will make substantial improvements in weather support at the CCAFS/KSC.

## References


Bellue, D.G., B.F. Boyd, W.W. Vaughn, J.T. Madura, T. Garner, K.A. Winters, J.W. Weems, and H.C. Herring, 2006: Shuttle weather support from design to launch to return to flight. 12th Conf. on Aviation, Range and Aerospace Meteorology, Atlanta, GA, Amer. Meteorol. Soc., paper 8.1 (CD-ROM).

Boyd, B. F., W. P. Roeder, D. Hajek, and M. B. Wilson, 2005: Installation, Upgrade, and Evaluation a Short Baseline Cloud-to-Ground Lightning Surveillance System in Support of Space Launch Operations, *1st Conference on Meteorological Applications of Lightning Data*, 9-13 Jan 05, 4 pp.

Brody, F.C., R.A. Lafosse, D.G. Bellue, and T.D. Oram, 1997: Operation of the National Weather Service Spaceflight Meteorology Group, *Weather and Forecasting*, **12**, 526-544

Biagi, C.J., K.L. Cummins, K.E. Kehoe, and E.P. Krider, 2007: National Lightning Detection Network (NLDN) performance in southern Arizona, Texas, and Oklahoma in 2003-2004. *J. Geophys. Res.*, **112**, doi:10.1029/2006JD007341.

Harms, D.E., B.F. Boyd, F.C. Flinn, T.M. McNamara, J.T. Madura, T.L. Wilfong, and P.R. Conant, 2003: Weather system upgrades to support space launch at the Eastern Range and the Kennedy Space Center. 12th Symp. on Meteorological Observations and Instrumentation, Long Beach, CA, Amer. Meteorol. Soc., paper 7.1 (CD-ROM).

Lang, T, et al., 2004: The Severe Thunderstorm Electrification and Precipitation Study. *Bull. Amer. Meteorol. Soc.*, **85**, 1107-1125.

Lennon, C. and L. Maier, 1991: Lightning mapping system. 1991 Int'l. Aerospace and Ground Conf. on Lightning and Static Elec., NASA Conf. Pub. 3106, paper 89-1.

Orville, R.E. and G.R. Huffines, 2001: Cloud-to-ground lightning in the United States: NLDN results in the first decade, 1989-1998. *Mon. Wea. Rev.*, **129**, 1179-1193.

Roeder, W. P., and T. M. McNamara, 2006: A Survey Of The Lightning Launch Commit Criteria, *2nd Conference on Meteorological Applications of Lightning Data*, 29 Jan-2 Feb 06, 18 pp

Roeder, W. P., J. W. Weems, and P. B. Wahner, 2005: Applications Of The Cloud-To-Ground-Lightning-Surveillance-System Database, *1st Conference on Meteorological Applications of Lightning Data*, 9-13 Jan 05, 5 pp.

Thomas, R.J., P.R. Krehbiel, W. Rison, S.J. Hunyady, W.P. Winn, T. Hamlin, and J. Harlin, 2004: Accuracy of the Lightning Mapping Array. *J. Geophys. Res.*, **109**, doi:10.1029/2004JD004549.

Thottappillil, R., V.A. Rakov, M.A. Uman, W.H. Beasley, M.J. Master, and D.V. Shelukin, 1992: Lightning subsequent stroke electric field peak greater than the first stroke peak and multiple ground terminations. *J. Geophys. Res.*, **97**, 7503-7509.

Valine, W.J. and E.P. Krider, 2002: Statistics and characteristics of cloud-to-ground lightning with multiple ground contacts. *J. Geophys. Res.*, **107**, doi:10.1029/2001JD001360.

**Disclaimer**

Mention of a copyrighted, trademarked, or proprietary product, service, or document does not constitute endorsement thereof by public employee author(s) or the U.S. Government. Any such mention is solely for the purpose of fully informing the reader of the resources used to perform the work reported herein.


Figure 1. Map of sensor sites in original LDAR (open triangles) and 4DLSS (filled squares).

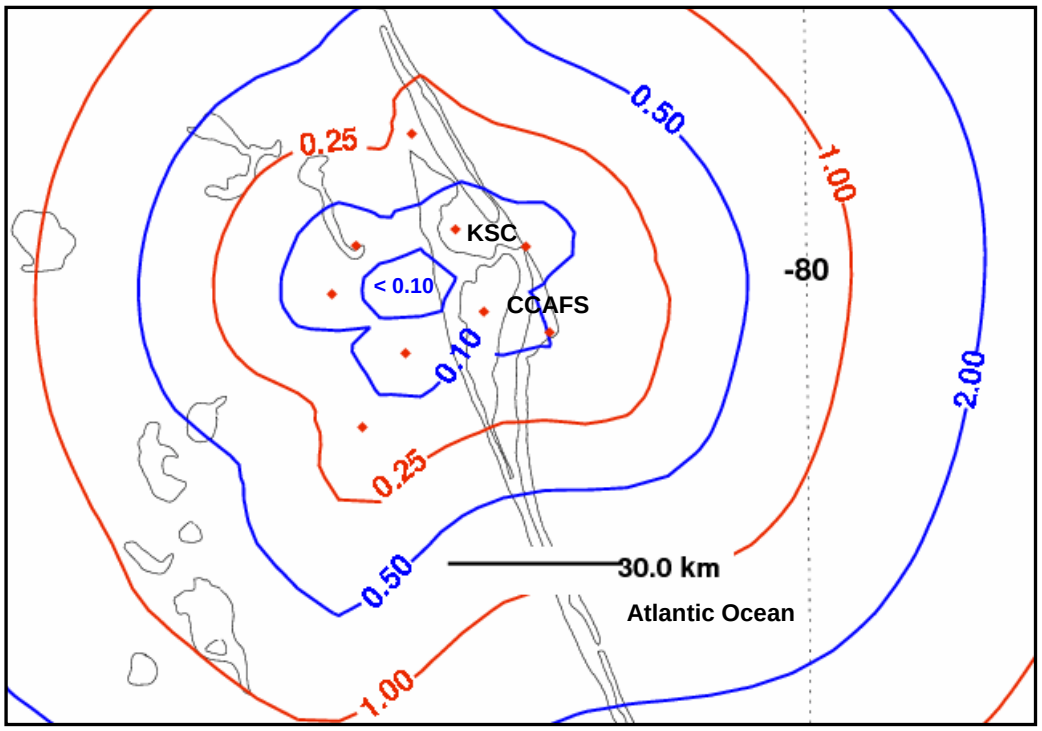


Fig. 2. Modeled location accuracy of 4DLSS, in km. Value represents median (50%) accuracy, that is, half of the locations are closer to the real position than the value shown here and half are farther away. Red dots are sensor sites. Plot is zoomed in on the CCAFS/KSC complex area.

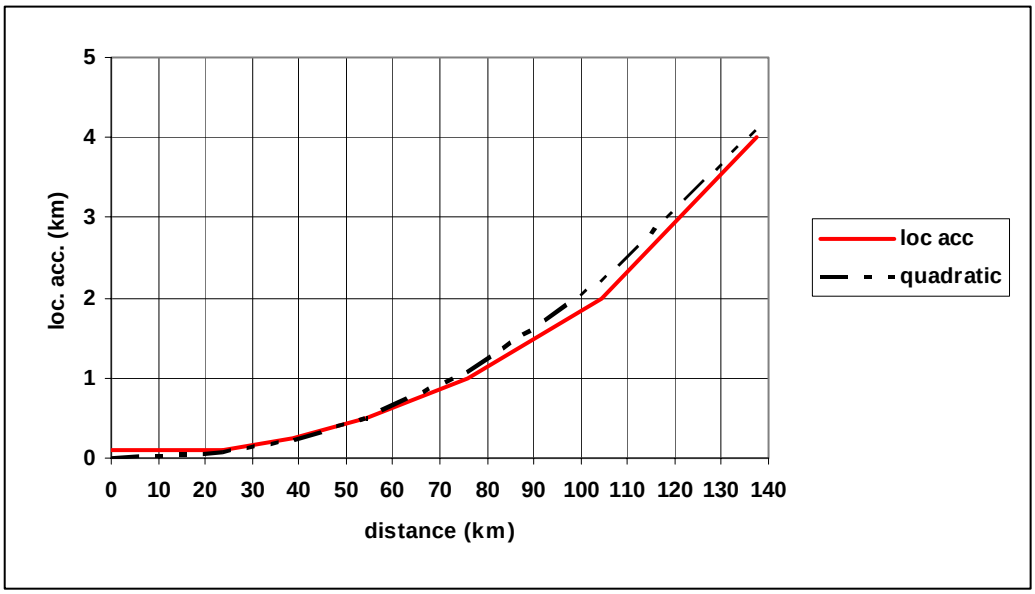


Fig. 3. Summary of values in Fig. 2 as a function of distance from the center of the network. The approximately quadratic fit to the modeled location accuracy values is $LA = (6*10^{-5})d^{2.2747}$ where d is distance in km. The $R^2$ value for this empirical fit is 0.9988.

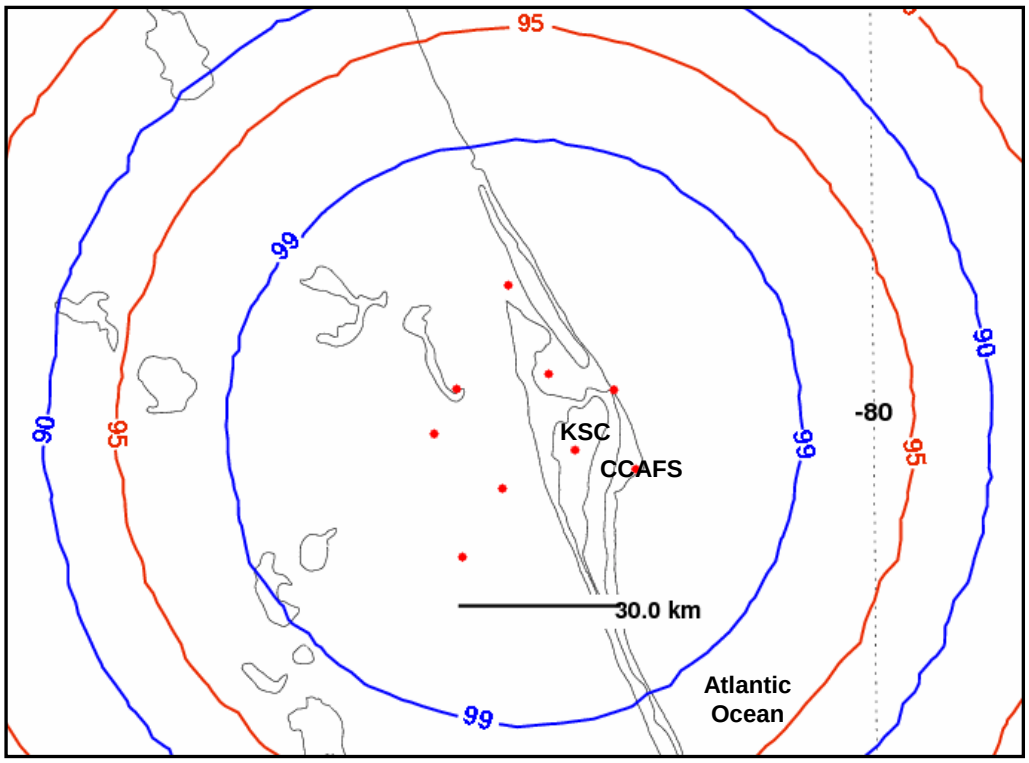


Fig. 4. Modeled flash detection efficiency of 4DLSS, in percent. Red dots are sensor sites. Plot is zoomed in on the CCAFS/KSC area.

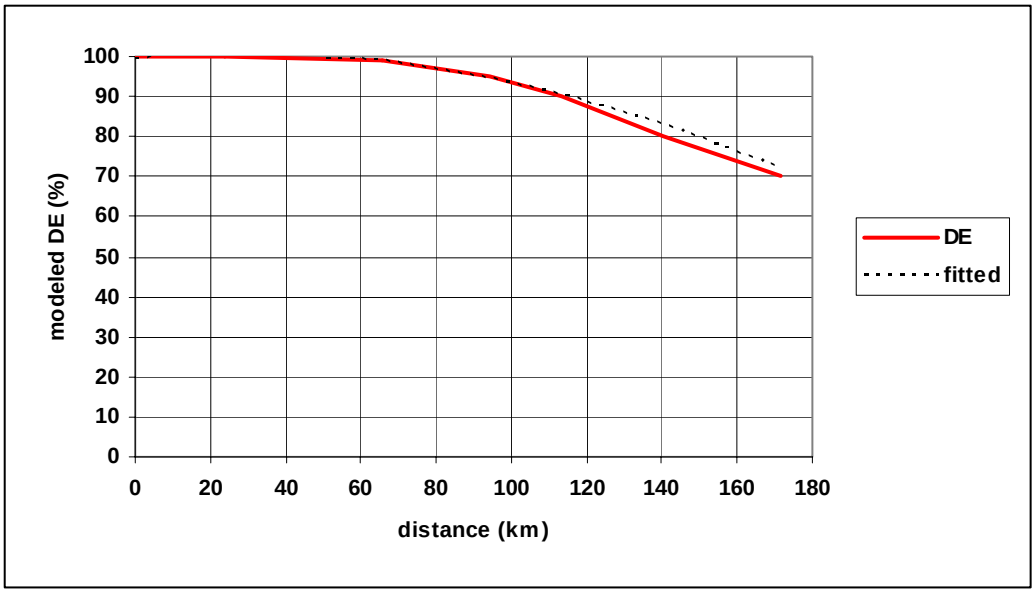


Fig. 5 Summary of Fig. 4 as a function of distance from the center of the network. An empirical best fit to this curve is DE = $-0.0014d^2 + 0.0786d + 99.69$, where "d" is distance in km. The $R^2$ value for this empirical fit is 0.9967.

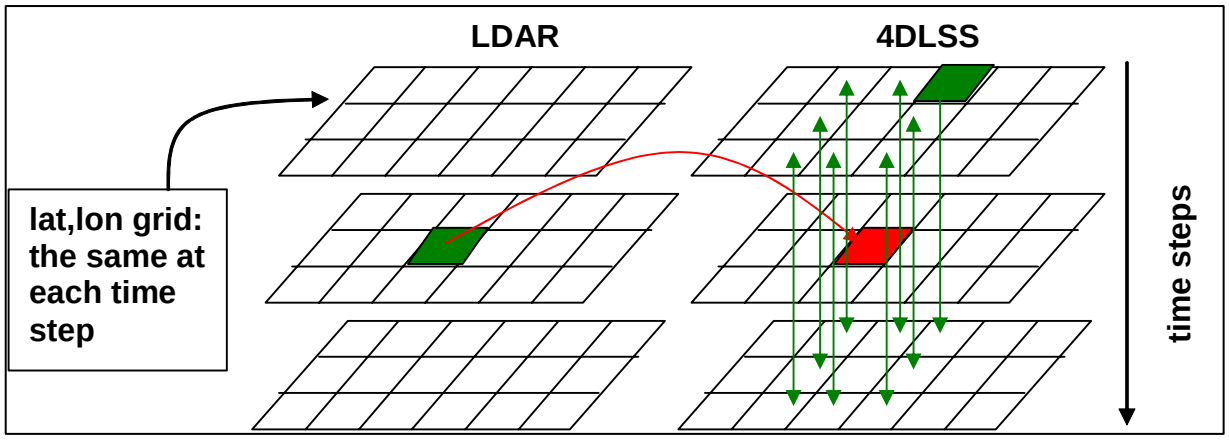


Fig. 6. Illustration of automated comparison algorithm. At a given time step, we compare the same grid cell between the two networks (red arrow), and then we also search in surrounding grid squares plus and minus one time step (green arrows).

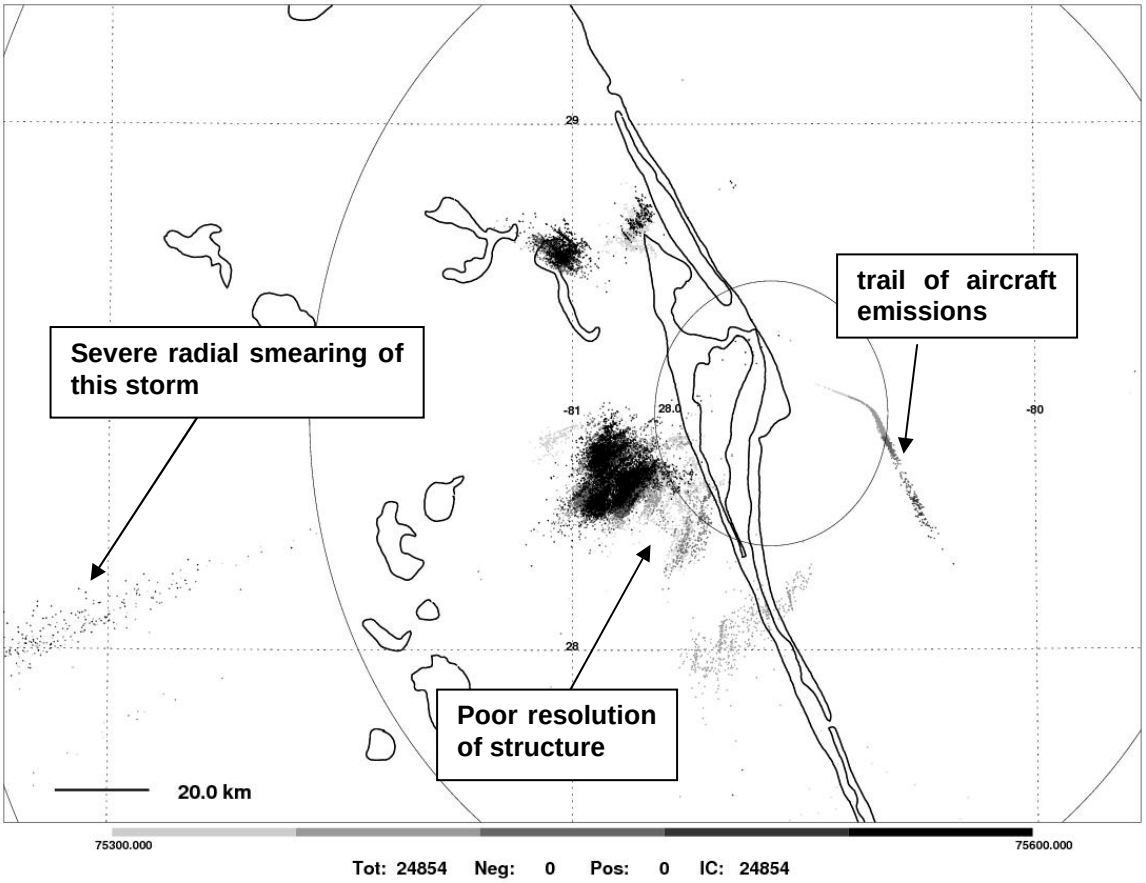


Fig. 7a. LDAR data for 20:55-21:00 Z on 21 September 2007, shown in the 5-color grayscale format used by the operational CCAFS/KSC LDAR display (most recent one minute is in black, and data from previous minutes is in successively lighter shades of gray). Several features are pointed out for comparison with Fig. 7b (below).

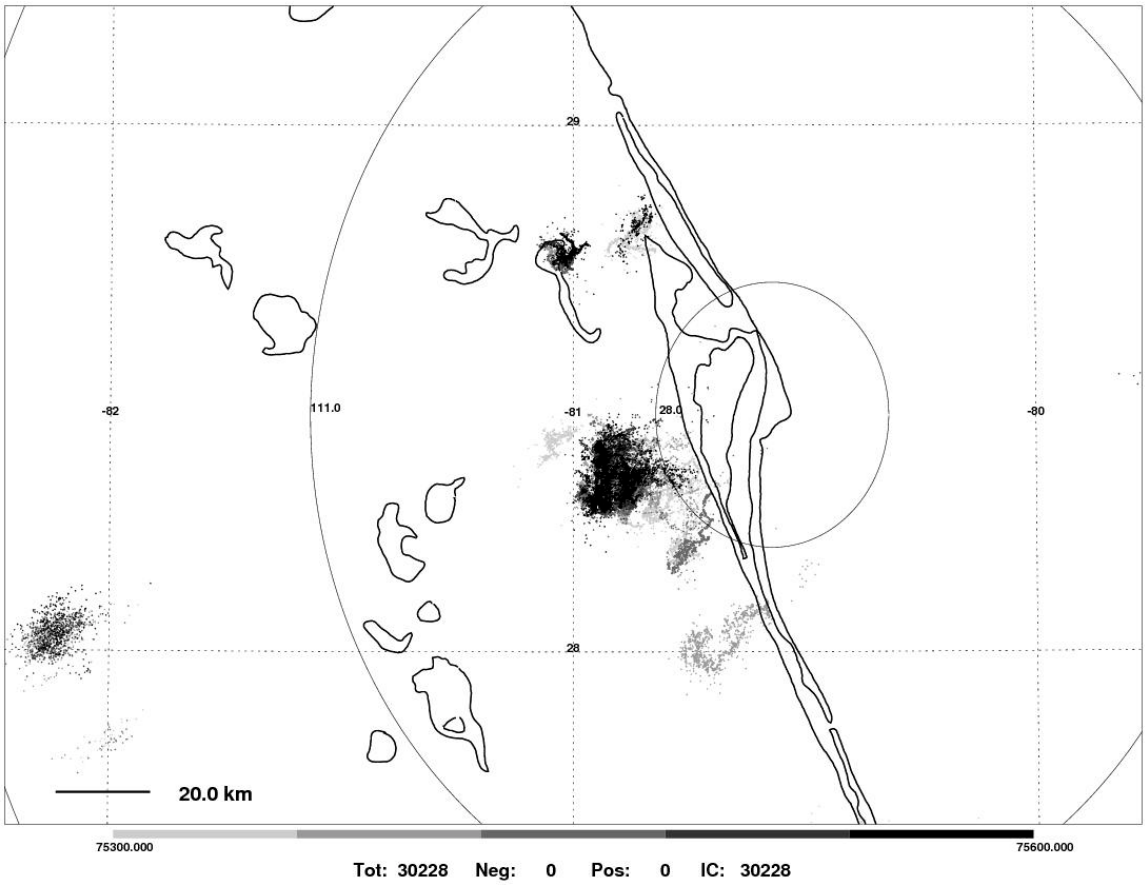


Fig. 7b. 4DLSS data for the same five-minute period as shown in Figure 7a.

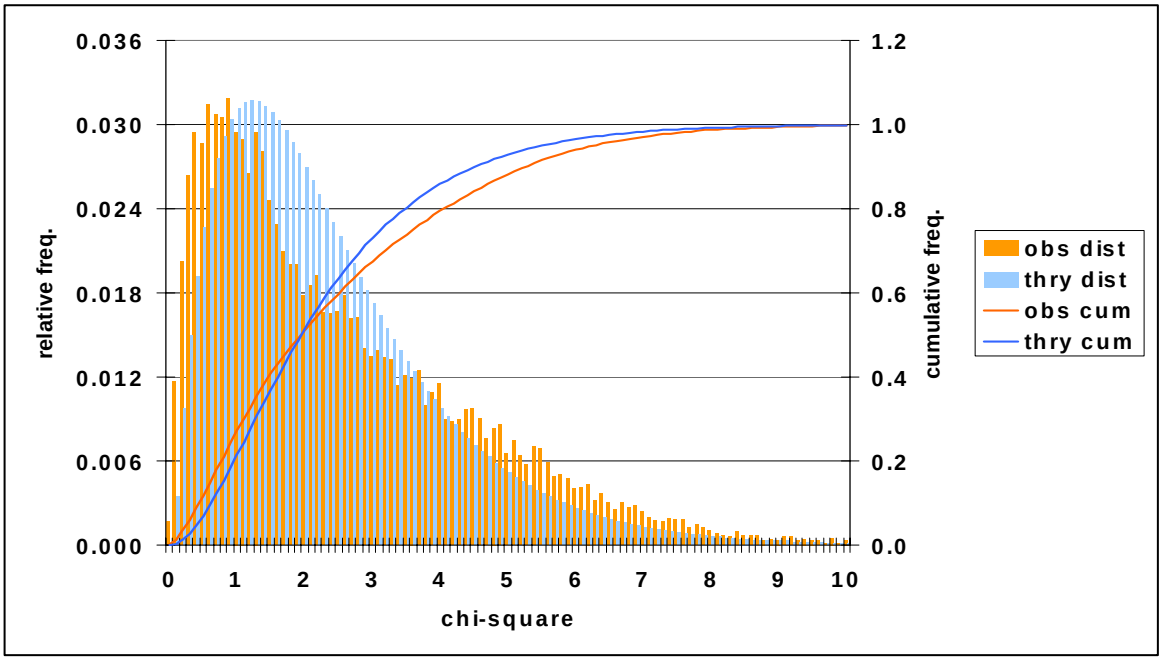


Fig. 8. Chi-square analysis. Observations in orange, theoretical in blue. Distributions are referenced to left-hand axis, cumulative distributions to right-hand axis.

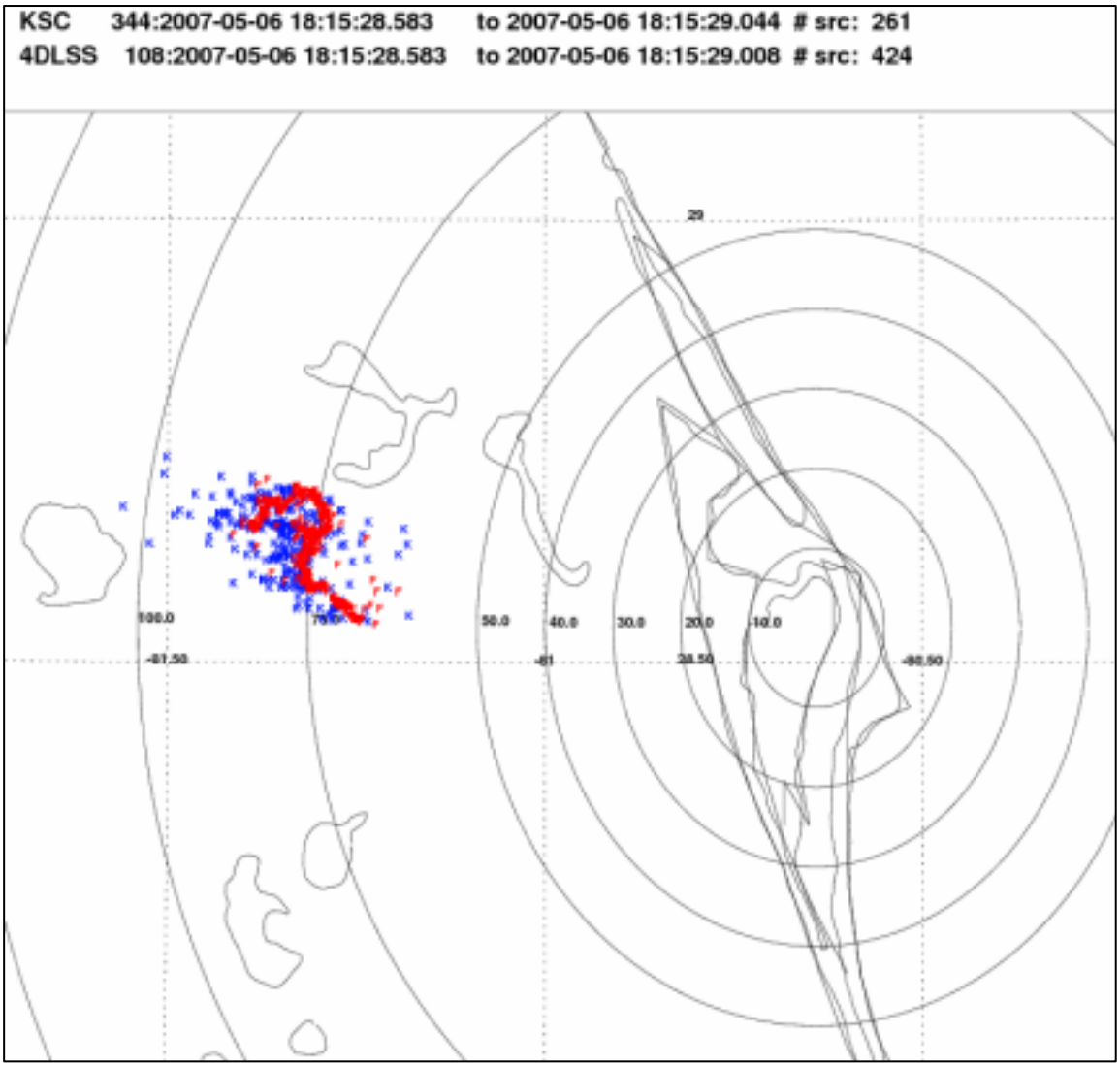


Fig. 9. Original LDAR (blue) and 4DLSS (red) for a flash at about 75 km from KSC/CCAFS on 6 May 2007. Note the reduced radial location errors in the 4DLSS data, leading to a more natural branch-like appearance for this lightning flash.

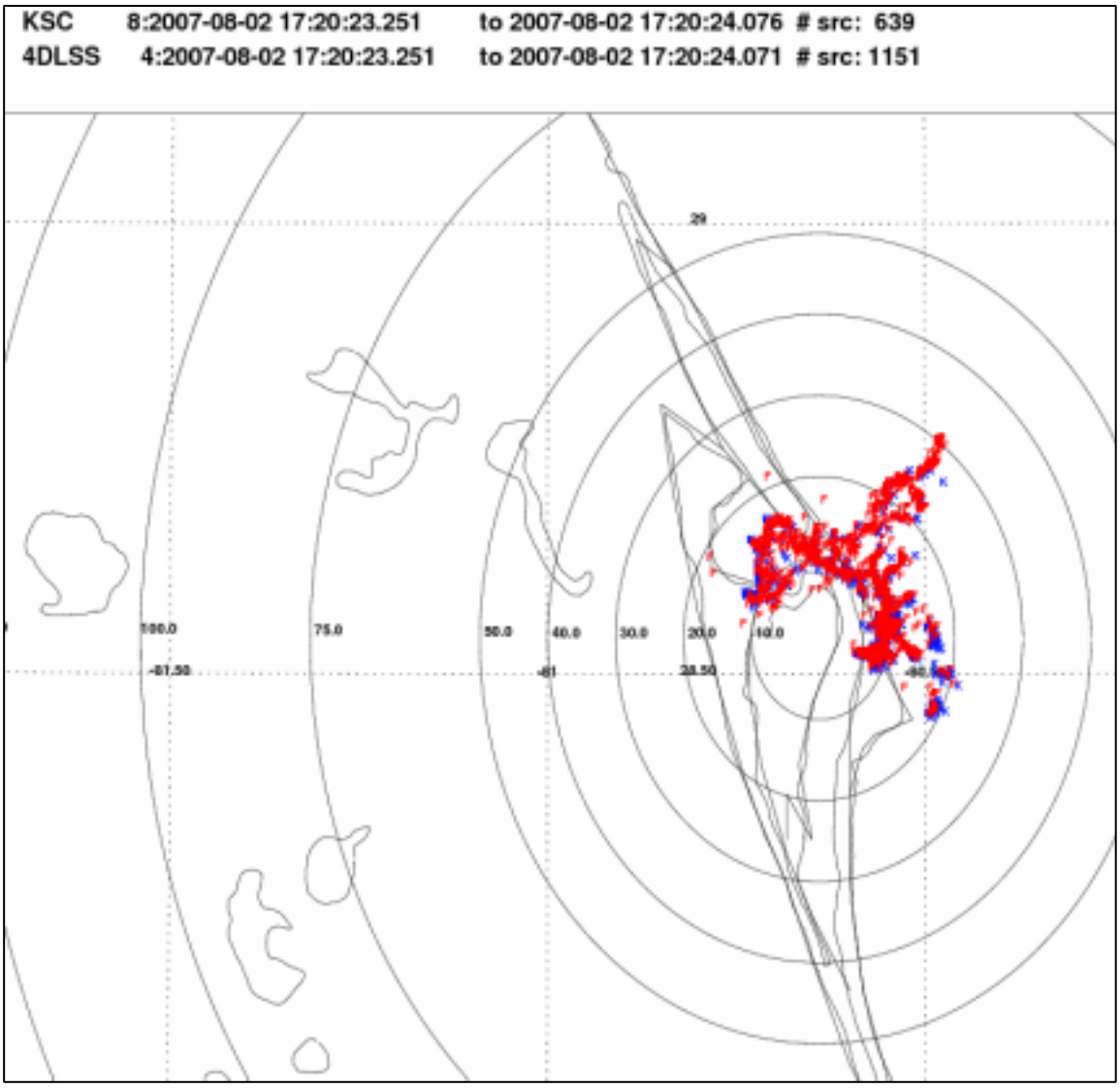


Fig. 10. Original LDAR (blue) and 4DLSS (red) for a lightning flash over the KSC/CCAFS complex on 2 August 2007. Note the excellent spatio-temporal correlation between the 4DLSS and LDAR data.

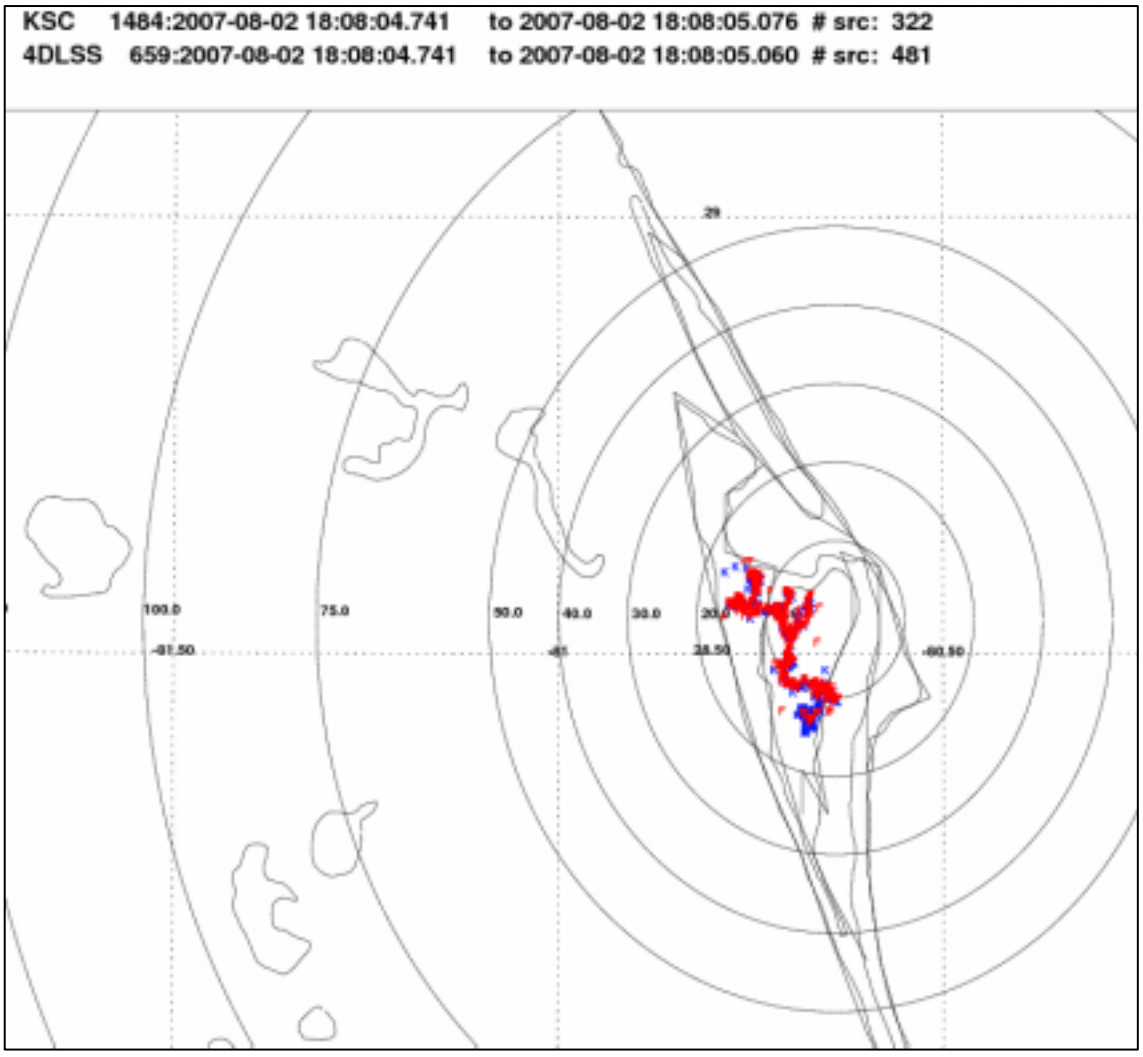


Fig. 11. Original LDAR (blue) and 4DLSS (red) for a lightning flash over the KSC/CCAFS complex on 2 August 2007.

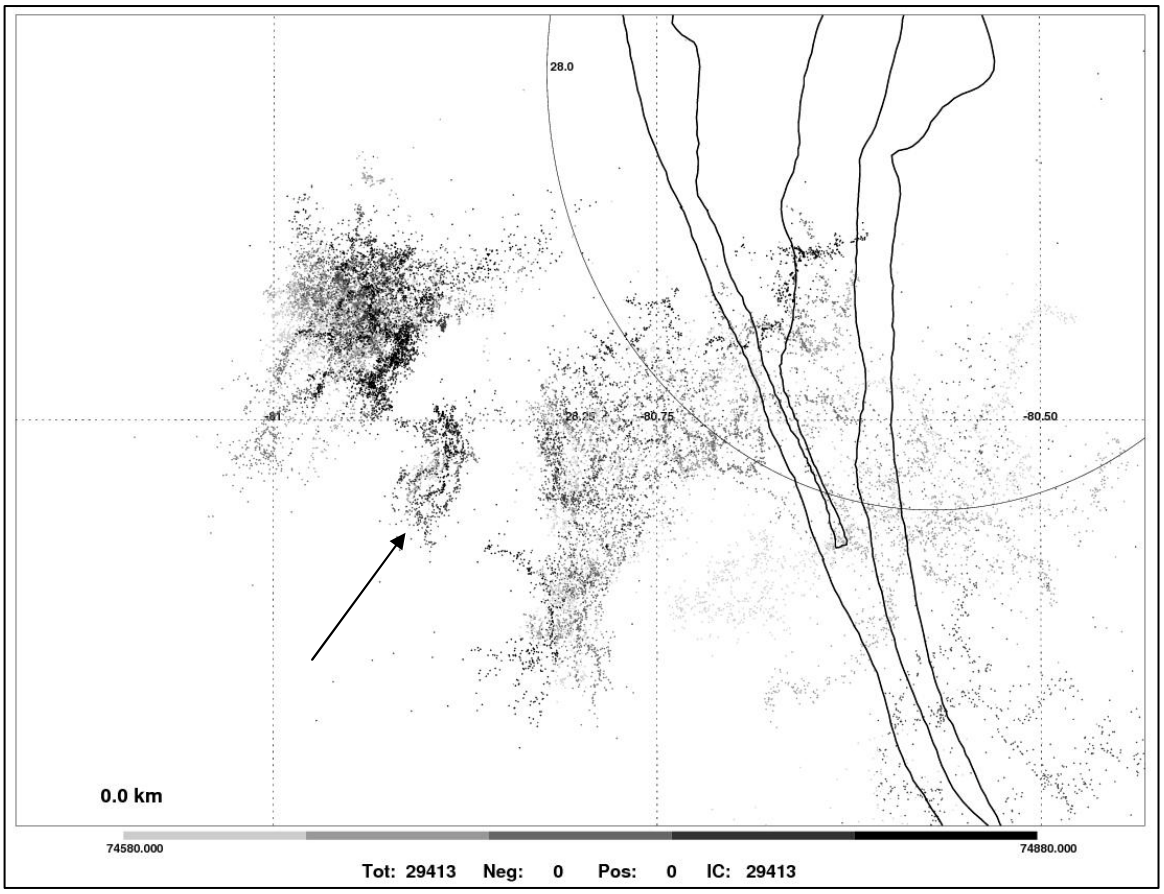


Fig. 12a. 4DLSS data from 21 Sept. 2007, 20:43-20:48 GMT. Arrow points to small-scale gaps in lightning flashes. These gaps were believed to be "lightning holes", a potential indicator of severe weather. This storm went on to produce tornadoes.

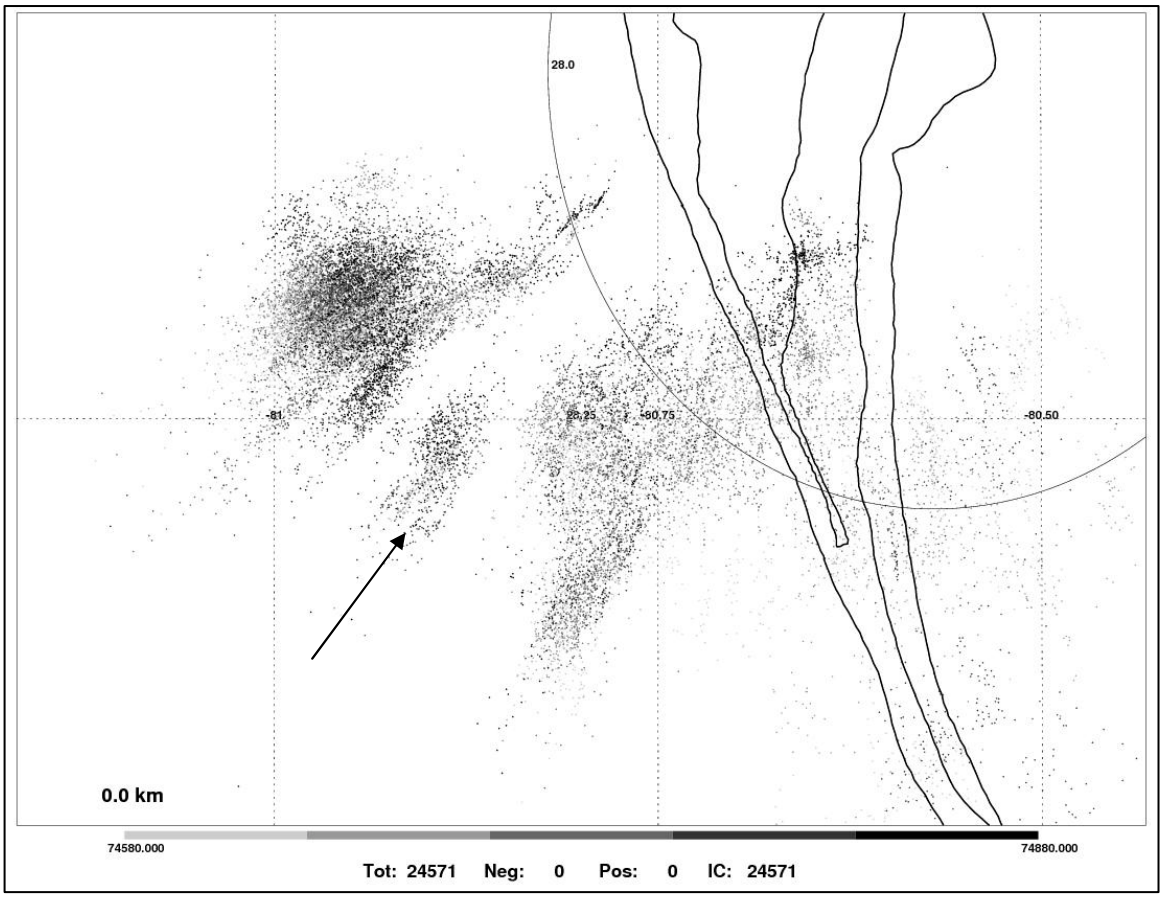


Fig. 12b. Original LDAR for the same time period as Fig. 12a. Note that the radial smearing of the LDAR data obscured the possible "lightning holes" observed in the 4DLSS data near the tip of the black arrow.

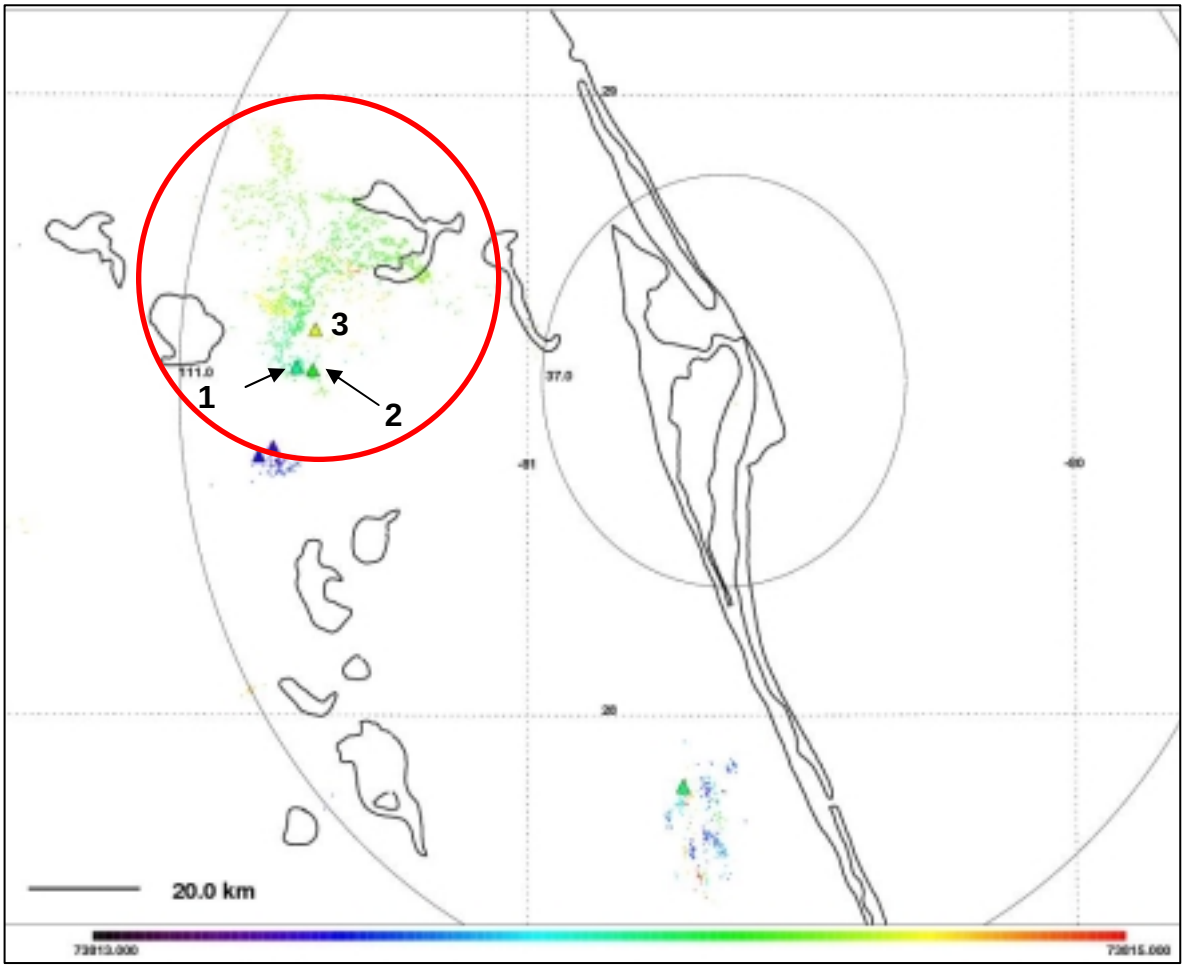


Fig. 13. Long horizontal flash (circled) with three CG strokes on 6 May 2007. Small dots are VHF sources detected by 4DLSS. Color-filled triangles are CG strokes. The order of the strokes is shown by 1,2,3. The color scale represents time, with the left edge (dark purple) at 20:30:13 GMT and the right edge (red) at 20:30:15. The same color scale applies to VHF sources and CG strokes.